Nuclear Instruments and Methods in Physics Research B 371 (2016) 12–26

Contents lists available at ScienceDirect

Nuclear Instruments and Methods in Physics Research B

journal homepage: www.elsevier.com/locate/nimb

50 years of ion channeling in materials science

André Vantomme

Instituut voor Kern- en Stralingsfysica, KU Leuven, Celestijnenlaan 200 D, B-3001 Leuven, Belgium

ARTICLE INFO

Article history:
Received 19 August 2015
Received in revised form 26 November 2015
Accepted 26 November 2015
Available online 28 December 2015

Keywords:
Ion channeling
Material science
Crystallography
Defects and impurities
Rutherford backscattering spectrometry

ABSTRACT

In the early days of ion beam analysis, i.e. the early 60s, channeling was discovered and brought to maturity via a combined effort in experimental, computational and theoretical research. It was soon realized that the probability for nuclear interaction (such as nuclear scattering, nuclear reactions, ionization followed by X-ray emission...) would significantly decrease when steering the ion beam along a crystallographic direction of a single crystal. Hence, this effect would be optimally suited to investigate a wide range of materials properties related to their crystal structure, such as defects, elastic strain, the lattice site of impurities, as well as phonon-related properties.

In this paper, I will briefly review some of the pioneering work, which led to the discovery and theoretical understanding of ion channeling. Subsequently, a number of applications will be discussed where the strength of the ion beam analysis technique allows deducing information which is often hardly (or not) attainable by other techniques. Throughout the paper, I will reflect on the future of channeling in materials research, and pay special attention to potential pitfalls, challenges and opportunities.

1. Introduction

When nuclear physicists started abandoning their small accelerators in the sixties, research activities in ion-beam/solid interactions were booming. Among others, it was discovered that energetic charged particles can be steered through a single crystal over a long distance, without undergoing any large-angle scattering. This effect, well-known as (ion) channeling, is nowadays a well-established technique to assess basically any material property which is related to (a deviation of) its crystal structure. A channeling experiment benefits from the same depth, elemental, isotopic... sensitivity as the ion beam analysis technique it relies on, e.g., Rutherford backscattering spectrometry, particle-induced X-ray emission, nuclear reaction analysis... Since its discovery, a variety of channeling approaches have been developed and applied in a wide scala of materials science studies, and meanwhile, the technique is routinely used to investigate defect densities and depth distributions, lattice sites of impurities, elastic strain, etc.

At the occasion of the Ion Beam Analysis 2015 conference, the rich history of channeling during the past 50 years has been reviewed. In this paper, a brief overview will be presented on how channeling was first discovered, subsequently combined with emerging ion beam analysis techniques, and finally came to full maturity. A number of important milestones and pioneering papers will be highlighted, emphasizing the impact they had within the community. Next, a selection of applications of ion channeling will be illustrated, paying particular attention to some of the less-known – but extremely nice – work that optimally exploited the strength of the technique. Along that line, specific attention will be paid to potential pitfalls, weaknesses and strengths of channeling, future opportunities, etc.

This paper is not aimed to review the full theory and all experimental details of channeling (for which the reader is referred to the many excellent textbooks and review papers written during the past decades, even as early as the 70s), but will focus on how it all started and illustrate that – despite the very carefully conducted early experiments – many details and potential pitfalls have meanwhile unfortunately been forgotten. Furthermore, I will dwell on a number of the paramount advances, which brought along the strength of the ion channeling technique, even beyond its standard use. These include examples where ion beam analysis has been driven to its extremes, where the experiment was performed under exotic conditions, or where non-conventional schemes or approaches were used – including progress in the experimental set-up and in simulations of the channeling effect. Moreover, I will reflect on the future of ion channeling during the decades to come. It is anticipated that channeling will remain competitive with and complementary to other characterization techniques providing (local) structural information, including synchrotron-based approaches and state-of-the-art electron microscopy.

http://dx.doi.org/10.1016/j.nimb.2015.11.035
0168-583X/

Selecting a (limited) number of important experiments and milestone achievement during these 50 years is a nearly undoable task – many more could (and should) have been included in this paper. The final result is a personal selection, which definitely leaves out a lot of fascinating work. These examples focus nearly entirely on axial channeling of ions, thus largely leaving out planar channeling (which can be extremely powerful for specific applications, but is experimentally more challenging and theoretically less developed) and the use of other charged particles such as electrons, positrons, muons, etc.

2. The discovery of channeling

2.1. How it all started

Although channeling – i.e. the steering of charged particles through high-symmetry directions of a crystal, in Lindhard's words – was discovered and developed approximately 50 years ago, it could actually have been 100 years. In the early 20th century, M. von Laue along with W.H. Bragg and W.L. Bragg tried to understand the spotty patterns which were observed when an X-ray beam was scattered from a crystal. At the time, they were not aware yet of the wave nature of X-rays, so an explanation was sought using the concept of light-particles (photons) passing through the crystal along open "channels" between the atomic rows, a phenomenon they called "Kanalisierung", i.e. the German word for channeling (Fig. 1). Within this context, the near-discovery of channeling came soon after, in 1912, when Johannes Stark published his ideas on scattering and absorption of β-rays and X-rays in crystals [1]. In this paper, based on his previous experiments [2], he conjectured that "ion rays" could penetrate deeper into the interior of a crystal when they are parallel to specific planes.

Although Stark wanted to investigate this transmission of β-rays and X-rays through crystals, he mentioned that he was unable to do so at that time, but proposed which experiments needed to be done and claimed that these considerations should be applicable to α-radiation as well. However, the idea was not picked up, and channeling remained unnoticed for another half century. In particular, since the Bragg's showed that X-ray diffraction is an interference effect, rather than related to channeling, the entire "channeling concept" got abandoned, even to the extent that the early (coincidental) observations of channeling in the late 50s were interpreted in terms of diffraction [3].

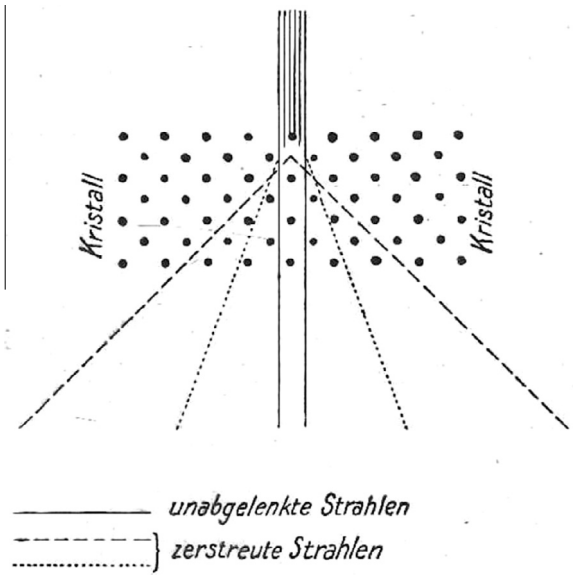

Fig. 1. The "Kanalisierung" experiment as suggested by Stark, illustrating non-deflected and scattered beams. Reproduced from [1].

2.2. The first observations of channeling

In the early days of implantation, a lot of effort was put in determining depth profiles of both the implanted species and the induced defects, and in measuring sputter yields. Quite often, these studies were performed in the framework of "materials for nuclear applications" projects, with emphasis on keV-energies and a broad scope of projectile masses. In a number of reports, a clear evidence of crystallographic effects on the implantation process showed up. On the one hand, upon irradiation with 20 keV Ar or Ne, Rol et al. [4,5] observed variations of the sputter yield of single crystalline Cu with varying crystal orientation. Similarly, in their high-energy sputtering experiments of *fcc* Cu, Nelson and Thompson found strongly preferred directions for the ejection of atoms, which they assigned to "momentum focusing" [6]. On the other hand, when investigating the depth profile of implanted ions, Davies and Sims observed inconsistencies with theory and with other experimental data [7]. In particular, both Bredov and Okuneva [8] and Davies, McIntyre and Sims [9] studied the depth profile of 4 keV implanted Cs in Ge. To determine the profile, they implanted radioactive ^{137}Cs and measured the remaining activity in the sample after consecutive etching steps. Surprisingly, the profiles measured by Bredov and Okuneva were orders of magnitude deeper than those found by Davis, McIntyre and Sims, the latter agreeing well with the LSS treatment. At the time, the authors did not realize that Bredov used a single crystalline target, whereas Davies' sample was amorphous, thus putting channeling forward as the most likely explanation. Subsequently, the depth profiles of several ion/target combinations were measured, many of them exhibiting a small exponential tail extending very deep in the target (see Fig. 2) [7,9].

Until then, attempts to explain this behavior focused on "increased transparency" or alike phenomena. However, a crucial step forward was made by Robinson and Oen, who simulated the trajectory of keV Cu recoils in Cu, similar to those which are induced by neutron bombardment of a Cu substrate. In their computer simulation using structure-less targets, no signs of an exponential tail were found. Conversely, when switching to crystalline targets (Fig. 3), the first clear evidence of channeling was found – and was first explained in terms of "Coulombic steering" – and presented at a conference in Paris in 1961 [10,11].

Very soon after, three groups independently produced experimental confirmation of the computationally predicted channeling effect. At Chalk River National Lab, depth profiles of radioactive ^{85}Kr implanted in polycrystalline and single crystalline Al were compared when implanting along several crystal directions [13]. On the other hand, in Munich, a similar approach was used for studying ^{85}Kr in Cu profiles [14]. The observed "tunnel focusing" or "super range effect", as the authors named it, confirmed the results predicted by Robinson and Oen's computer simulations. The third experimental confirmation, at Harwell, was based on a different approach. Nelson and Thompson measured the transmission of 50 keV protons through a very thin single crystalline Au foil, as a function of azimuthal (to keep the path length of the beam unaltered) rotation angle of the foil [15]. They found that the transmission significantly enhanced at specific angles, when the beam lined up with a ⟨110⟩ axis, and this effect was shown to remain even for energies in the MeV range, hence in the electronic stopping regime [16]. The latter was an important step in expanding channeling towards the regime of interest for *ion beam analysis*, whereas all previous efforts had focused on low-energy heavy ions,

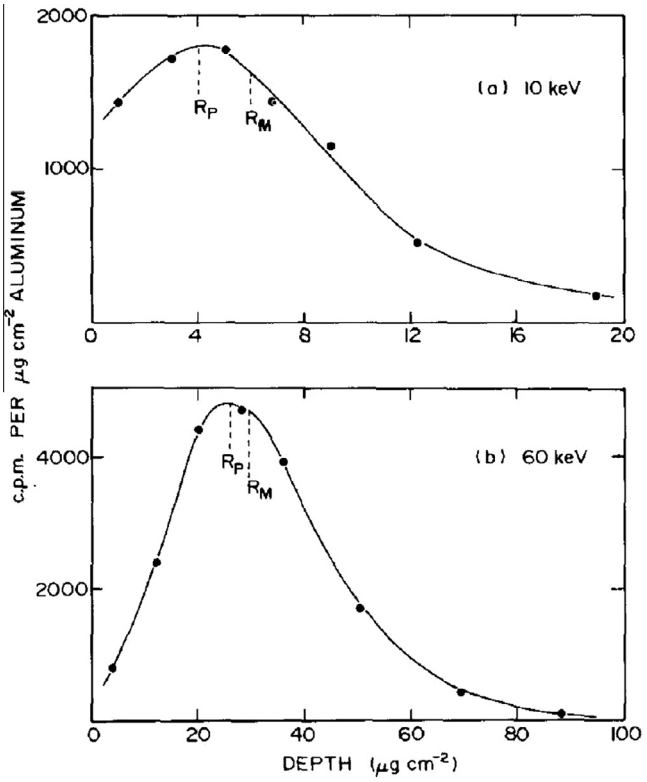

Fig. 2. Depth profile of 10 keV (a) and 60 keV (b) ^{24}Na ions implanted in aluminum, showing a prominent tail deep in the substrate. Reproduced from [7].

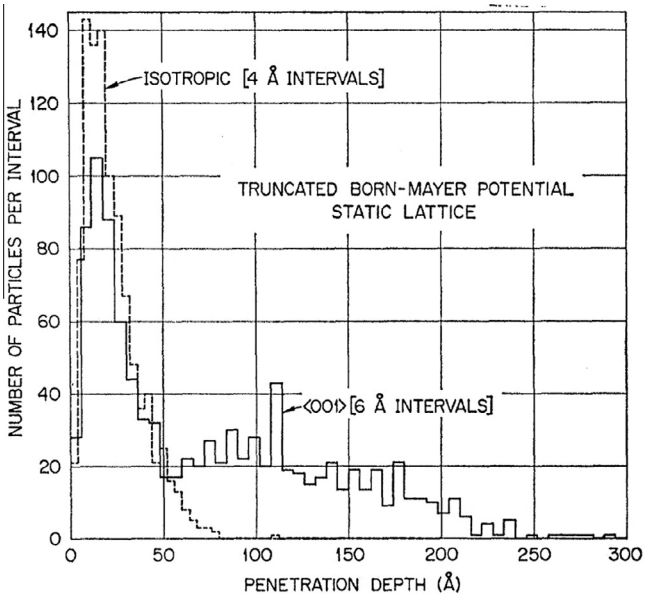

Fig. 3. Depth distribution for 5 keV Cu ions on *fcc* Cu, for isotropic and ⟨0 0 1⟩ incidence. Reproduced from [12].

i.e. typical implantation conditions. Although some potential objections to explaining the above results by the channeling concept could still be brought up, they were a more than firm support.

2.3. The era of channeling

Now that the first indications of channeling were found, things could really take off. Actually, the real emergence of channeling happened in 1964 in Aarhus, which was, according to John Davies, the "channeling explosion" [3]. In just a couple of months, ion channeling was explored both theoretically and experimentally, and nearly all major parameters governing the channeling phenomenon were revealed. Looking back at it now, it was probably a matter of (the coincidence of) having the right people together at the right time at the right place. In 1964, Davies spent a sabbatical in Aarhus, and brought his experimental data on implanted ion ranges (many of them revealing an asymmetric profile with a pronounced exponential tail), a manuscript by Dearnaley on channeling in the high-energy electronic stopping regime and a set of good single crystals, allowing detailed experimental channeling studies [3]. Triggered by the experimental observations of channeling, Jens Lindhard started investigating this phenomenon theoretically, allowing him to present his theoretical framework in a matter of merely two months and publishing his substantial channeling paper one year later [17]. An important step in his approach was to implement the concept of a continuum potential suggested a year earlier by Lehmann and Leibfried [18] and Nelson and Thompson [15], i.e. "smearing out" the potential of a row of atoms, rather than considering collisions with individual atoms.

On the one hand, Lindhard's theory provided two important and commonly used equations, i.e. for the critical angle ψ_1 and minimum yield $\chi_{\min}$, as well as the channeling/blocking reversibility.

$$\Psi_1 = \sqrt{\frac{2Z_1Z_2e^2}{dE}} \tag{1}$$

$$\chi_{\min} \approx \pi a^2 dN \tag{2}$$

In these equations, Z_1 and Z_2 are the atomic number of the particle and substrate atom, respectively, e is the elementary charge, E the ion energy, a the Thomas–Fermi screening length, N the atomic density of the target, and d the interatomic spacing along the direction of the ion beam. In the same seminal paper [17], Lindhard already introduced the concept of the *Rutherford shadow behind one atom* (i.e. the shadow cone) and the resulting redistribution of ions away from the string of atoms. As a final comment on [17], it should be mentioned that Lindhard emphasized the importance of thermal vibrations of the string atoms, as a "deviation from the perfect lattice". These vibrations have to be taken into account when evaluating the string potential, and may eventually reduce the channeling effect at high temperature, i.e. resulting in a higher $\chi_{\min}$ and smaller ψ_1. However, Lindhard pointed out that 'in measurements including changes of temperature, it should be possible to verify positions of ions in the lattice and even check vibrations'. Examples of temperature dependent channeling measurements will be discussed in Section 3.7.

On the other hand, the theoretical predictions triggered the attention of experimentalists to the fact that the yield of violent collisions in nuclear processes could be a handle for quantitatively studying ion channeling – rather than focusing on implantation profiles as had been mostly done so far. Indeed, since a channeling ion experiences fewer violent collisions with target atoms, one expects a lower probability for nuclear interactions, whatever the nature of these interactions is – thus affecting sputtering, the range of ions (nuclear stopping), nuclear reactions such as (p,γ) and (p,n), ionization and X-ray emission, (back)scattering... As a consequence, the yield of sputtering, of NRA (nuclear reaction analysis), PIXE (particle-induced X-ray emission), RBS (Rutherford backscattering spectrometry)... is expected to drop accordingly.

In July 1964, Bøgh, Davies and Nielsen developed a very simple goniometer (using a long pointer to read out the angle) to study the angle-dependence of the 405 keV (p,γ) nuclear reaction on ^{27}Al. The measurement revealed a significant reduction in reaction rate when aligning the proton beam with the ⟨1 1 0⟩ axis of the aluminum crystal – now referred to as 'angular scan' (Fig. 4). Their

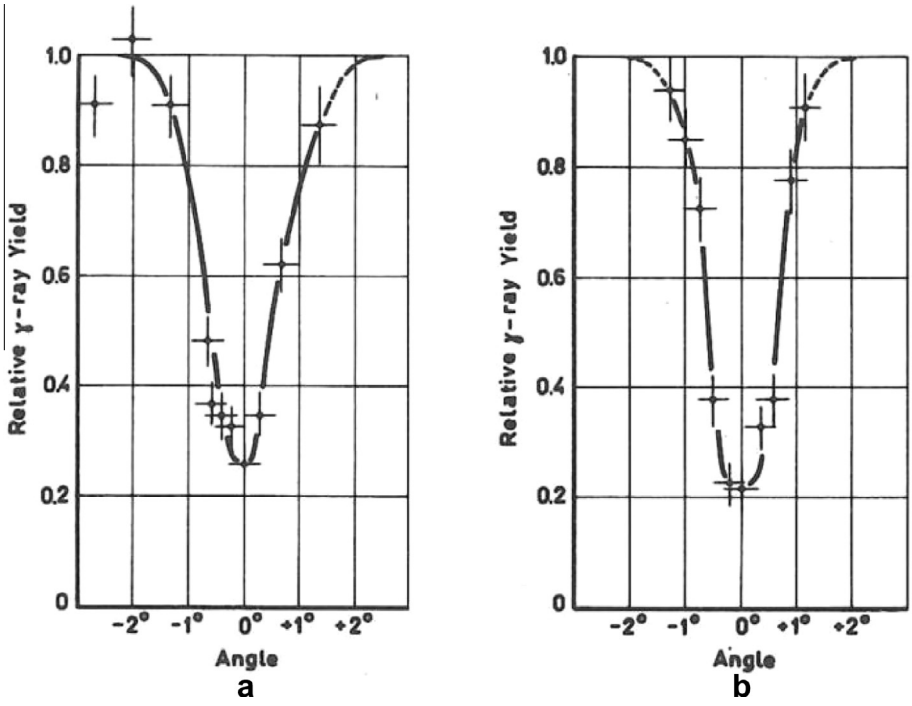

Fig. 4. The ^{27}Al(p,γ) yield versus the angle between the incident proton beam and the ⟨1 1 0⟩ axis, for horizontal (left) and vertical (right) tilting. Reproduced from [20].

experimental findings were in good agreement with Lindhard's theory, in particular when taking the simple experimental conditions into account. As such, this can probably be considered the first ion beam analysis channeling experiment in our current understanding of this terminology.

Both the experimental results by Bøgh et al. and the theory by Lindhard were simultaneously submitted to Physics Letters by the end of August, and published as back-to-back papers mid-September [19,20]. For completeness, it should be pointed out that Mike Thompson performed similar experiments at about the same time [21], using a (p,γ) reaction on Cu, later followed by several groups exploring other approaches of channeling, such as using α emitting implanted ions [22] or proton-induced X-ray emission [23].

Although the discussion so far focused on channeling of the ions of an external beam incident on a single crystal, Lindhard's theoretical treatise [17] already included the *rule of reversibility*: channeling of a charged particle from an external beam (which provides the probability of hitting a nucleus in the crystal) is equivalent to the reversed process, i.e. channeling of particles emitted by atoms located in the strings of the crystal (providing the angular distribution of emitted particles outside the crystal). Hence, the latter approach – referred to as blocking – is equivalent to channeling. This equivalence was not only theoretically investigated from the very beginning, but also experimentally. Indeed, already in 1965, blocking experiments using particles emitted upon implantation of radioactive ions into a single crystal [24], particles scattered from a single crystal [25] or both [26] proved the validity of the reversibility principle and significantly helped in advancing the understanding of channeling. For a review on channeling/blocking of ions, electrons and positrons, their recent advances as well as their applications, the reader is referred to [27].

The discovery of ion channeling coincided with the breakthrough of RBS, and it became immediately clear that the latter technique would offer ideal flexibility (in terms of a wide selection of energies, atomic numbers, depth sensitivity…) to systematically investigate the channeling behavior. In 1965, i.e. 50 years ago at

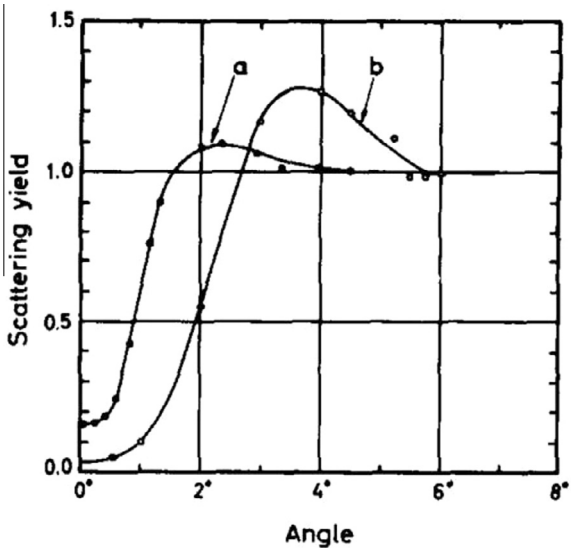

Fig. 5. Scattering yield as a function of the angle between a 400 keV proton beam and the Al ⟨1 1 0⟩ (a) and Ta ⟨1 0 0⟩ (b) axis. Reproduced from [29].

the time of the 22nd international conference on *Ion Beam Analysis*, the first RBS/channeling experiments were done by Bøgh and Uggerhøj using 400–1700 keV proton beams and Al and Ta single crystals (Fig. 5) [28,29]. Their early reports confirmed the critical angle predicted by Lindhard [19] and that the ions remain channeled deep in the crystal.

3. Channeling applications

After three exciting years, packed with pioneering experiments and revealing fascinating new physics of ion–solid interactions, it had become clear that channeling could be exploited to investigate a wide variety of materials properties, all of them related in some

way to (a deviation of) the material's crystalline structure. Undoubtedly, this transition was largely driven by James W. Mayer. In the mid-60s, he investigated doping of semiconductors by ion implantation, trying to unravel the observed relations between the implantation/annealing temperature and the dopant efficiency/distribution. Jim Mayer and John Davies joined forces in investigating the behavior of ion-implanted silicon, particularly using RBS/channeling. Within just a couple of years, they brought the application of channeling in materials science to maturity, hence their work played a decisive role in bringing channeling to a new community [3].

In the remaining part of this paper, a selection of examples will be reviewed, some of them being famous textbook examples, whereas others remained less well-known despite their importance. Given the context of the *Ion Beam Analysis* conference, the selected applications will largely deal with ion *beam* applications (hence using an external ion beam), with particular focus on RBS. The reader is referred to the outstanding books and reviews that have been written on channeling for a broader overview of channeling applications.

3.1. Efficiently observing channeling

Before taking off with the channeling examples, a comment is made on the efficient detection of ion channeling. Throughout these 50 years, the vast majority of the experiments have detected the angular dependence of a nuclear process by performing a large number of consecutive measurements using a slightly different alignment of the sample with respect to the ion beam (or the angle between the sample and the detector in case of blocking experiments), i.e. constructing an *angular scan*. Hence, a large number of measurements is needed in order to construct a one-dimensional profile, a very time consuming exercise. However, from the very beginning, "position-sensitive detectors" (PSD) have been used in channeling studies, more precisely a photographic plate to observe the entire "proton plot" of the crystal [25,30]. The advantage is twofold: on the one hand, all information is captured at once rather than needing to repeat the measurement for various alignments; on the other hand a full two-dimensional pattern is obtained, offering more complete information compared to a one-dimensional scan. Obviously – and unfortunately – fluorescent screens do not provide any quantitative data. Therefore, this approach got largely abandoned and it lasted approximately until the 90s for a new generation of PSD's to make their entrance in channeling. However, the relatively limited energy resolution for MeV α detection which was available in those days largely limited their use to emission channeling (see below), rather than RBS/channeling [31–33]. In a joint effort with nuclear scientists, there has been renewed interest recently in using both pixel-based detectors and resistive charge division photodiodes [34], hopefully paving the way towards easier and high-throughput blocking/channeling studies with a good energy resolution.

3.2. (Radiation) damage

Probably one of the most frequently-used applications of ion channeling is the study of defects in crystal lattices. This approach, brought to maturity in the 60s through investigations of implantation-induced defects in semiconductors (as discussed above – see, a.o. Ref. [35]), actually applies to damage generated in any way, e.g., upon ion implantation or irradiation, upon thin film growth, after thermal treatment... As an example, Fig. 6 shows the random and ⟨1 1 1⟩ aligned backscattering spectra for germanium implanted with 40 keV In to various fluences [35]. The area under the "surface" peak (channels 75–82) is a direct measure for the number of displaced Ge atoms. As clearly revealed

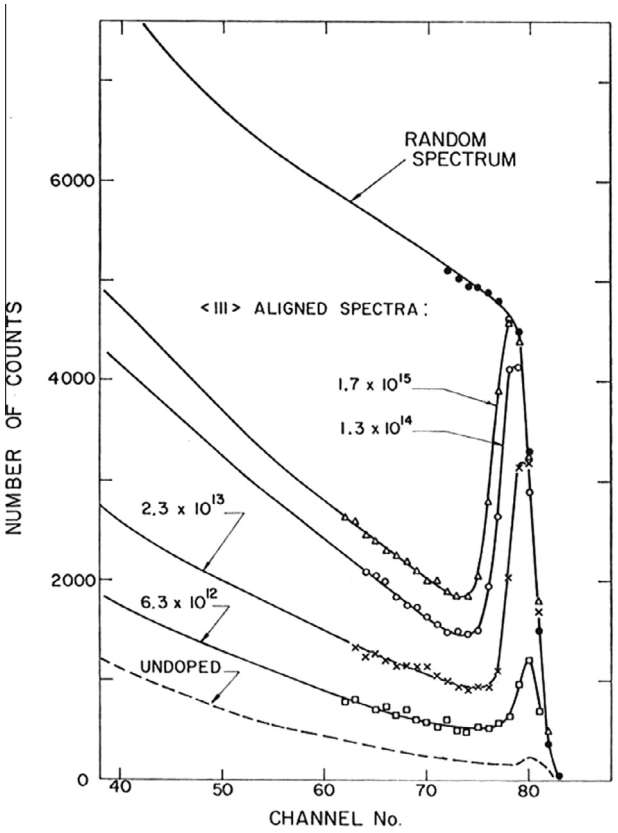

Fig. 6. 1 MeV He^+ random and ⟨1 1 1⟩ aligned spectra for Ge implanted at room temperature with various fluences of 40 keV In ions. Reproduced from [35].

from the channeling spectra, this fraction of displaced atoms increases with increasing implantation fluence, until finally reaching the random level, indicating all Ge atoms have been displaced from their lattice site (i.e. amorphization).

A specific strength is that channeling spots every (even slightly – as little as ~0.1 Å) displaced atom, and that quantitative and direct information is obtained without the need for neither complex modeling nor for working in reciprocal space. Moreover, as opposed to many other techniques used in defect studies, channeling benefits from the inherent depth resolution and mass selectivity of RBS, or the element and isotope sensitivity of PIXE and NRA, respectively. On the other hand, two drawbacks are that one merely detects that the atoms are displaced, and that the information is averaged over the entire beam spot area. Quite often, more detailed qualitative information is required by the materials scientist, hence extra information with other (complementary) approaches must be obtained. As illustrated by a vast amount of reports, the combination of channeling with, a.o., TEM (transmission electron microscopy) or XRD (X-ray diffraction), often proves to be an ideal marriage.

Going back to the early days, it is striking how extremely detailed and carefully the pioneering studies were performed [35,36]. This will be illustrated by briefly discussing three experimental aspects. First of all, already then it was realized that a proper conversion of the energy of the backscattered ions to a depth scale is only obtained when taking the different (electronic) stopping power in channeling geometry into account. Indeed, Erginsoy et al. showed that the stopping power in random and aligned geometry can differ by more than a factor of two [37]. Based on Bohr's equipartition rule, they suggested that this reduction in electronic energy loss is mainly due to the lower number of close impact-type collisions for a symmetric direction. Obviously,

one should realize this is a non-trivial problem, since with increasing damage, the stopping power will *gradually* increase from its value along a channeling direction towards the random value.

A second important issue dealt with in early experiments is the fact that (back) scattering (or any other nuclear interaction) can occur after (i) hitting a displaced atom, or (ii) when colliding with a substitutional atom after an incoming ion was dechanneled in the damaged region. Only the former provides information on the defect fraction, hence the latter (i.e. the dechanneling fraction) must be subtracted from the experimental spectrum in order to assess the defect density. A direct consequence of the dechanneling is that the backscattering yield originating from the undamaged (deeper) part of the crystal (channels 60–75 in Fig. 6) does not exhibit the low level expected for undoped germanium. As seen from the figure, the yield in this deeper region increases with increasing defect concentration in the near-surface region, i.e. increasing dechanneling of the incoming beam. To disentangle these two contributions to scattering, a procedure first suggested by Bøgh is typically used [38]. This approach basically constitutes a two-beam model, with the channeled beam yielding the defect density, and the random beam providing the dechanneled fraction, resulting in a simple equation to extract the defect density from the measured minimum yield:

$$\chi(x) = f_R(x) + (1 - f_R(x)) f \frac{n_D(x)}{N} \quad (3)$$

where $f_R(x)$ and $(1 - f_R(x))$ are the random and channeled fraction of the beam as a function of depth x, respectively, f is the defect scattering factor, N is the atomic density and $n_D(x)$ the defect depth profile [39].

Finally, the extracted defect fraction directly depends on the measured minimum yield, hence on the quality of the random spectrum that was captured. Although this may look a simple criterion to meet, great care should be taken to measure the random spectrum in a geometry far enough from the crystalline direction (to avoid the increased yield in the "shoulders") while avoiding minor channeling contributions, mostly as a result of partial planar channeling. Therefore, the random spectrum is ideally measured at least 5–7° away from the axis (in a direction that has the least impact on the energy-to-depth conversion), preferentially while keeping the sample azimuthally rotating throughout the measurement.

As mentioned above, all of these potential experimental pitfalls, i.e. (i) constructing a proper depth scale (using a reduced electronic stopping), (ii) subtracting the dechanneling fraction, and (iii) measuring a good random spectrum, were carefully taken into account in the early studies by a.o. Mayer and Davies [35,36], but are unfortunately often overlooked nowadays.

Whereas the defect depth profile can be quantitatively assessed by ion channeling, obtaining information on the nature of these defects is by far less straightforward. Although the different dependence of the defect scattering cross section on varying energy could in principle allow to identify defects [39], this approach is in practice far from ideal, in particular when several types of defects are simultaneously present. Alternatively, simulating the channeling energy spectrum can be much more beneficial and a number of efforts clearly underline how powerful this approach can be. As an example, I refer to the Monte Carlo simulations performed by Turos and co-workers [40]. Extending the approach originally outlined by Barrett [41], they used a binary collision model to simulate the channeling spectrum. Fig. 7 shows the results for a 2 MeV He beam channeling along the GaP ⟨100⟩ axis, for an ideally collimated ion beam (A), a beam divergence of 0.1° (B), and when increasing the vibration amplitudes (C–E). These simulations clearly show how minor variations in the sample

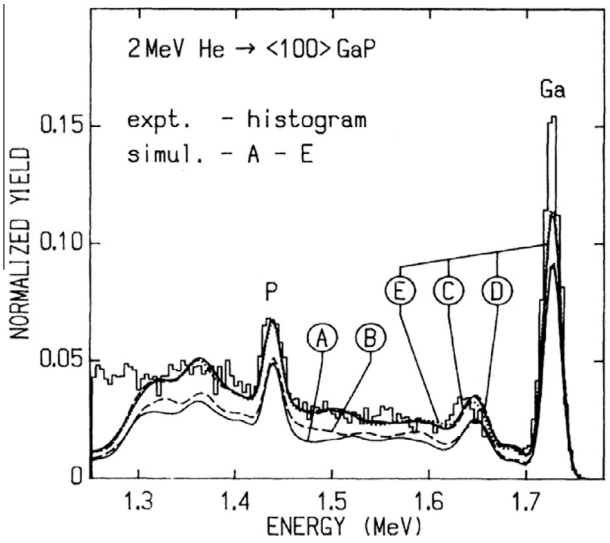

Fig. 7. Experimental (histogram) and simulated (curves) backscattering spectra for 2 MeV He ions channeled in ⟨100⟩ GaP. Reproduced from [40].

structure or the experiment can drastically change the channeling behavior.

Still, this code (and a number of similar attempts by other groups) only assumes randomly displaced atoms (RDA). On the other hand, McChasy (Monte Carlo CHAnneling SYmulation) [42] also takes dislocations into account. The power of this approach was illustrated for Ar implantation into a $SrTiO_3$ substrate for which the implantation depth profile was estimated by SRIM, a Monte Carlo code which simulates the stopping and range of ions in random media [43]. When considering only RDA's, an acceptable simulation of the channeling spectrum could only be obtained when assuming an unrealistically deep defect profile. On the other hand, allowing the presence of dislocations as well results in a very good fit which yields a depth distribution in good agreement with SRIM calculations [42].

A number of other IBA codes also attempt to simulate channeling spectra, such as RBX [44], BISIC [45]... For more details, the reader is referred to an IAEA intercomparison of IBA software [46]. However, the number of codes considering channeling is rather limited compared to the wealth of packages available for detailed simulation of random spectra. Moreover, these programs typically don't match the user-friendliness of their random counterparts either. Still, it is clear that this approach is very promising and potentially extremely powerful. Therefore, it is both a challenge and an opportunity to further exploit efforts in this direction. On the one hand, it may allow retrieving information on the nature of defects from a channeling spectrum (or alternatively, predicting the impact of a specific type of defects on the channeling behavior); while on the other hand it can be an important step towards directly linking the structural defects observed by channeling to those measured by other (also non-structural) characterization techniques.

From the above discussion, it is clear that channeling is ideal for quantitatively investigating defects, since the yield scales with the defect fraction. Conversely, one can wonder whether an increased yield necessarily points towards a defected crystal. Although one is inclined to answer positively, a beautiful study by Bai and Nicolet [47] shows that this is not necessarily the case. In particular, when dealing with a polyatomic crystal consisting of light and heavy atoms, such as $ReSi_2$, channeling along non-mixed rows (i.e. rows consisting of either Re or Si) has to be revisited. As a result of the much smaller critical angle along the Si rows compared to the

Re rows (see Eq. (1), which shows that ψ_c is proportional to the square root of the atomic number, i.e. 14 and 75 for Si and Re, respectively), there is a significant probability that ions dechannel from a Si atom after first impinging (and remaining channeled!) close to a Re column. The authors show – theoretically and experimentally – that this effect can drastically enhance the Si minimum yield (by a factor of up to 5) while leaving the Re minimum yield unaffected (Fig. 8). Hence it could lead to the erroneous conclusion that a large fraction of the Si atoms is displaced.

This "two-component model" has been extended to planar channeling, and applied to the case of epitaxial $ErSi_{2-x}$ layers of excellent crystalline quality [48]. In a similar way to axial channeling, mixed planes lead to a channeling behavior in accordance to the Lindhard formalism. On the other hand, for planes consisting of either only Er or only Si, a second component has to be added to the minimum yield. This component is very small for the Er signal, whereas the $(1\,0\,\bar{1}\,0)$ minimum yield for Si increases to 74%! In the case of $ErSi_{2-x}$, this effect is further enhanced by the presence of Si vacancies, and can even result in certain planar dips to completely disappear for the light element signal.

Finally, when assessing damage in single crystals, it is important to keep in mind that the extended ion irradiation required for the channeling measurements can induce defects itself. In this respect, ion beam analysis is not as *non-destructive* as often claimed. In particular for semiconductors, which are less resistant to irradiation damage than metals, a significant fraction of the defects generated during the ion bombardment do not recombine. Benzeggouta and Vickridge report on the damage accumulation in germanium and silicon upon a number of consecutive RBS/channeling measurements using a 1.57 MeV He beam [49]. After each measurement, a significant increase of the minimum yield is observed, in particular in the low-energy part of the spectrum. For silicon, a less radiation-sensitive material compared to germanium, this effect is by far less pronounced. However, even when no additional structural defects are observed after extended beam exposure (i.e. no increase of the minimum yield), one has to realize that other effects may manifest, such as elastic strain induced by the ion irradiation, or modification of the electrical, magnetic or optical properties [49].

Beam-induced defect accumulation is even more problematic for microbeam channeling, as reviewed by Jamieson et al. [50 and references therein] and Piette and Bodart [51]. Indeed, the extremely high fluence (up to 10^{19} He/cm^2) required to obtain statistically relevant data from a tiny area of the sample results in significant local defect fractions, yielding minimum yield values of 80% and above. Moreover, besides inducing defects in the host lattice, perturbation of the lattice location of impurity atoms (as discussed in detail in Section 3.5) may occur as well [50,52].

Besides defects induced in the sample interior, carbon buildup at the sample surface can occur as a result of the cracking of hydrocarbon molecules by the impinging energetic ions, a commonly known phenomenon when the scattering chamber is not equipped with oil-free vacuum pumps [49]. This thin carbon layer results both in an energy shift of the spectrum and in dechanneling of the ion beam, both of which directly affect the channeling measurement.

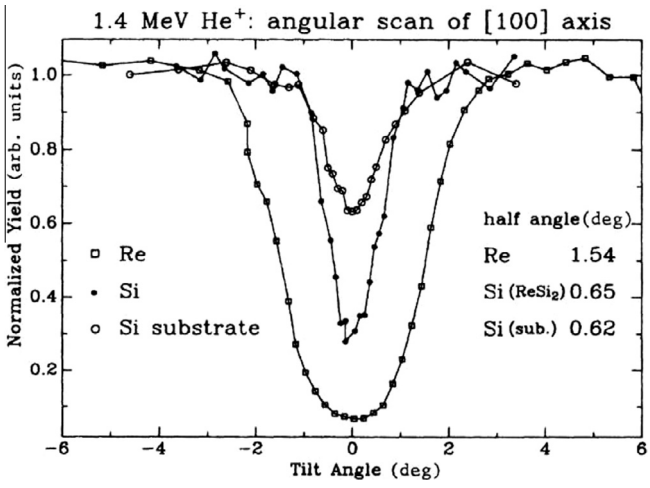

Fig. 8. Normalized backscattering yield as a function of tilt angle, showing a drastically enhanced minimum yield for the Si signal of the $ReSi_2$. Reproduced from [47].

3.3. Lattice structure

As explained above, a typical channeling measurement consists of measuring the variation in nuclear interaction yield as a function of the orientation between the ion beam and the crystal. Consequently, the position of and the mutual angles between the different crystalline directions (*in casu* crystal axes) can be determined – to a precision depending on the accuracy of the goniometer and the beam divergence. However, one can obtain more than just the location of these axes. The different interatomic spacing d along various axes will result in different critical angles for channeling, according to Eq. (1). As an example, Table 1 shows the normalized value of the interatomic spacing for the major axial directions of a number of simple cubic structures [53]. Since the critical angle is inversely proportional to the square root of d, the various axes can easily be distinguished, hence the lattice structure and orientation determined.

As can be imagined, such experiments are rather complicated and time-consuming. Since the same information can also be obtained much easier and faster (and often with higher precision) using diffraction techniques such as XRD, one may wonder why channeling should even be considered. However, once again, the depth and element selectivity of ion beam analysis can often outperform diffraction techniques. As an example, Dekoster et al. investigated the lattice structure of a 2 nm-thin Co film sandwiched between two Fe thin films [54]. Whereas bulk Co typically exhibits an *fcc* or *hcp* lattice structure, it was anticipated that the two adjacent Fe layers could stabilize Co in a *bcc* structure. The limited amount of material along with a nearly equal lattice constant of cubic Fe and cubic Co make XRD unsuitable to determine the Co lattice structure. Conversely, the ratio of the critical angles for channeling along the $\langle 0\,0\,1\rangle$ and $\langle 0\,1\,1\rangle$ direction, respectively, varies from 1.19 for *bcc* to 0.84 for *fcc*. The experimentally determined ratio of 1.23(4) for the Co signal (Fig. 9) clearly indicates that this 2 nm thin Co film assumes a metastable *bcc* structure.

3.4. Elastic strain measurement

As explained in Section 3.3, with a well-calibrated high-precision goniometer, one cannot only determine the nature of the axis, but the exact position as well, allowing the assessment of elastic strain (i.e. distortion of the lattice). In case of lattice-mismatched epitaxial thin films or multilayers, the elastic strain

Table 1
Normalized values of the interatomic spacing for the major axial directions of simple cubic structures [53].

Structure	$\langle 100\rangle$	$\langle 110\rangle$	$\langle 111\rangle$
fcc	1	$1/\sqrt{2}$	$\sqrt{3}$
bcc	1	$1/\sqrt{2}$	$\sqrt{3}/2$
NaCl	1/2	$1/\sqrt{2}$	$\sqrt{3}/2$

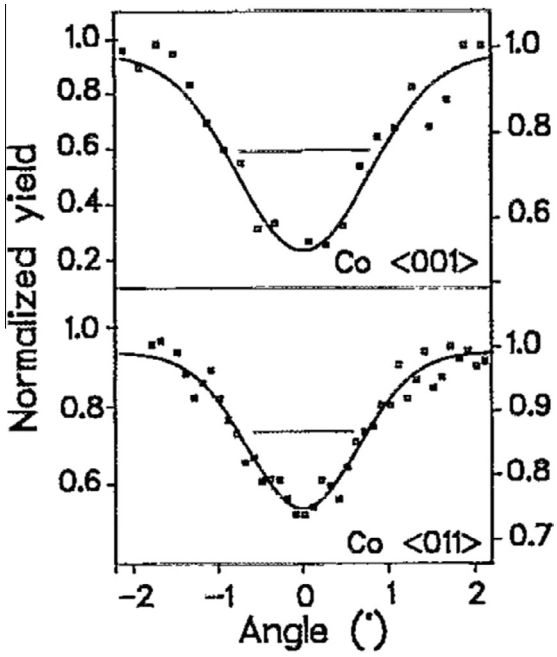

Fig. 9. Angular yield profiles for a 2 nm thin Co layer (in an Fe/Co/Co stack) along the ⟨001⟩ and ⟨001⟩ axis. Reproduced from [54].

in the film results in a minor shift of the position of non-normal axes. Fig. 10 schematically illustrates the example of a thin film with a cubic lattice, which is "forced" to adapt to a cubic substrate with a slightly larger lattice parameter. The angle with respect to the perpendicular direction can either increase (in case of tensile strain, as shown in Fig. 10) or decrease (for compressive strain). From a precise measurement of the angular change (the so-called kink angle, $\Delta\Psi$), the tetragonal distortion ε_T (i.e. the difference between the parallel and perpendicular elastic strain) can be directly determined:

$$\varepsilon_T = \frac{\Delta\Psi}{\sin\Psi_{sub}\cdot\cos\Psi_{sub}} \quad (4)$$

with Ψ_{sub} the angle of the non-normal axis with respect to the perpendicular direction for a relaxed lattice, i.e. $\Psi_{sub} = 35.26°$ for the ⟨110⟩ and the ⟨114⟩ axes shown in Fig. 10. This approach has already been demonstrated in the 80s, a.o. in studies of thin silicide layers [55,56].

Again, as was the case for the lattice structure, the question arises why one should not rely on the much simpler and more sensitive XRD technique. However, as opposed to RBS/channeling, XRD only provides information averaged in depth and it lacks element selectivity. The power of channeling is illustrated for a Si ⟨111⟩/$CoSi_2$/Si/$CoSi_2$/Si multilayer, for which XRD cannot distinguish between the two silicide layers, and neither between the Si top layer, interlayer and substrate. Moreover, the comparable lattice constant of Si and $CoSi_2$ further limits the sensitivity. On the other hand, RBS both separates the signals of Co and Si, and provides a depth profile (Fig. 11) [58].

When plotting the backscattering yield as a function of angle around the ⟨110⟩ and ⟨114⟩ axes (both 35.26° away from the ⟨111⟩ normal direction, one at either side), the axial position can be determined for every individual layer in the stack, revealing that both silicide layers are equally strained (tensile strain in the current example), whereas the thin Si layer in between the silicides is relaxed (Fig. 12).

Moreover, the very different critical angle (Eq. (1)) and minimum yield (Eq. (2)) allow to easily distinguish between the ⟨100⟩ and ⟨114⟩ axes. From Fig. 12, it is clear that the thickest silicide layer is fully aligned with the Si (i.e. it exhibits the same orientation for *all* crystal axes) whereas the thinnest film is azimuthally rotated by 180°, i.e. the ⟨100⟩ and ⟨114⟩ axis have changed positions. Obviously, this approach is not limited to multilayer stacks, but can also be applied to study the depth dependence of elastic strain in thick films or even in bulk samples, by simply using appropriate regions of integration when constructing the angular scans [59]. This approach has a depth sensitivity which is only limited by the inherent depth resolution of the ion beam technique that was used.

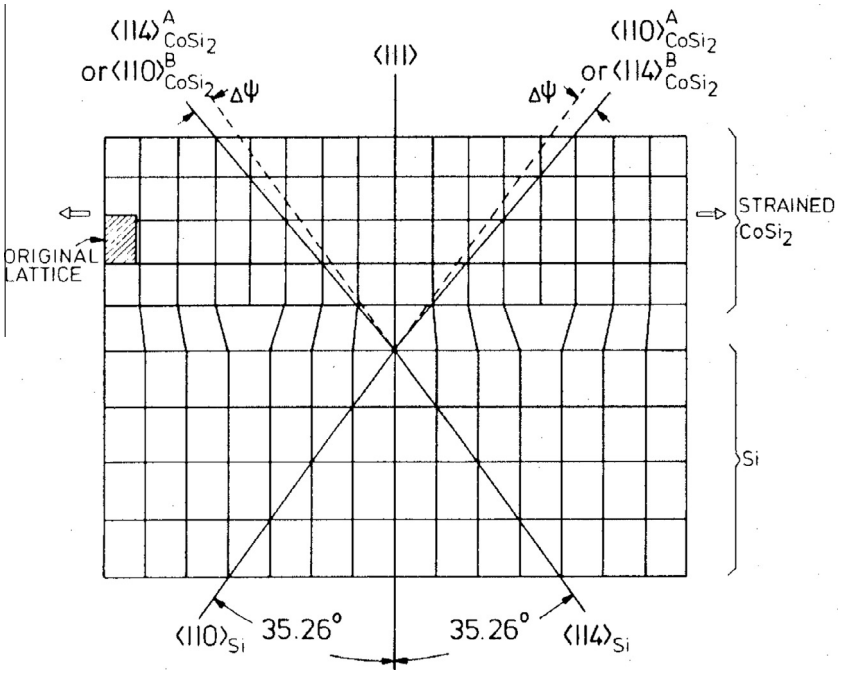

Fig. 10. Schematic diagram showing that the non-normal channeling axes of a (partially) strained thin film are misaligned relative to the corresponding axes of the substrate. Reproduced from [57].

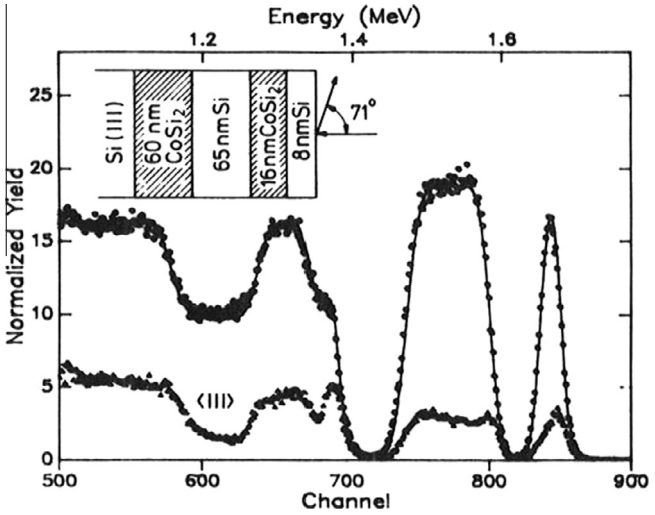

Fig. 11. Random and ⟨1 1 1⟩ aligned RBS spectra for a Si/$CoSi_2$ multilayer (see inset), allowing depth-dependent strain measurements. Reproduced from [58].

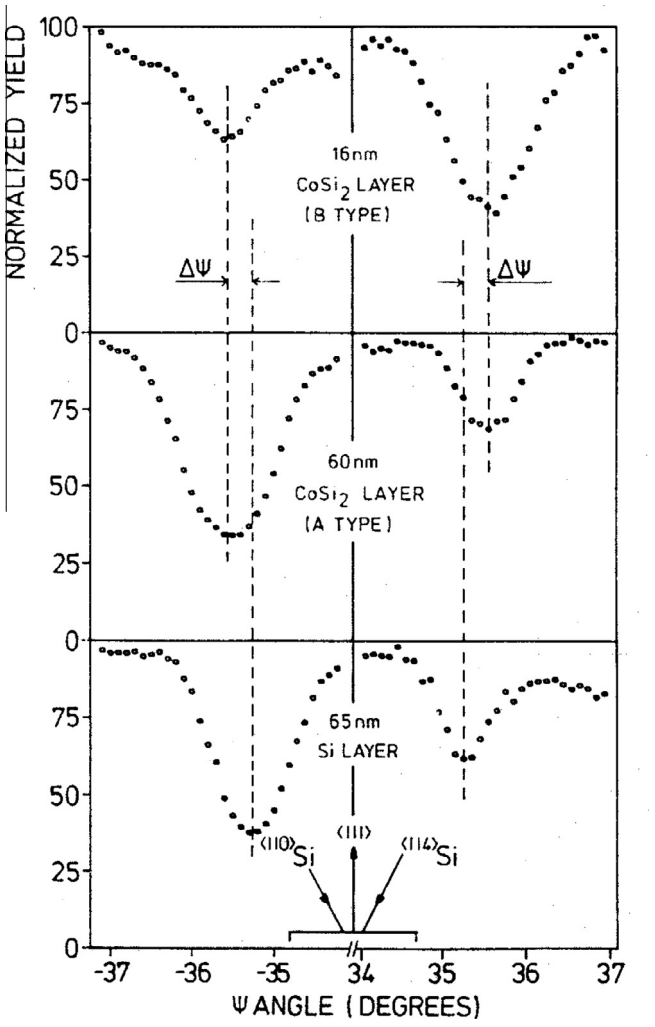

Fig. 12. Angular scans around the ⟨1 1 0⟩ and ⟨1 1 4⟩ axes for three layers of the sample from Fig. 11. Reproduced from [58].

Throughout the past decades, several attempts have been made to significantly enhance the sensitivity of channeling-based strain measurements. Without going into detail, I will just briefly refer to two of them. First, S.T. Picraux and W.K. Chu developed *catastrophic dechanneling* in strained-layer superlattices, involving a resonance between the planar channeling trajectory wavelength and the superlattice period [60,61]. At resonance, they observe a very abrupt (and complete) dechanneling at a specific depth, which is linked to the misalignment of the ion beam to the surface axis. With the use of a modified harmonic model, the strain is extracted with very good accuracy. In particular for superlattices lacking a high degree of perfection, this approach can compete with techniques as XRD and TEM [61]. On the other hand, Ijzendoorn and coworkers relied on the varying flux distribution as a function of the angle between the ion beam and the axis, to very accurately deduce the strain in *extremely thin* buried films [62,63]. The presence of this strained film results in a step in the substrate signal for channeling along a non-normal direction. From the dependence of the size of this step on the (small) misalignment from the non-normal axis, the strain can be very accurately determined. In both examples, the optimal *tuning of the ion flux* in the axis or plane is at the origin of the very high sensitivity of the strain measurement. Despite the very nice illustration of the physics of channeling, the complexity of such experiments has prevented their widespread use, and the reader is referred to the literature for further details on these models.

A final note on strain assessment with ion channeling concerns the impact of steering effects. In principle, when the ion beam is perfectly aligned with a non-normal axis of a lattice-mismatched thin film, no (or limited) channeling should occur in the substrate as a result of the kink angle, i.e. the ion beam is not aligned with the axial direction of the substrate. However, particularly for very high-quality, very thin films with a kink angle equal to or smaller than the critical angle, a major fraction of the ion beam is steered across the interface into the substrate axis [64,65]. Steering is particularly important at low energy, as a result of the larger critical angle (Eq. (1)). Although the steering effect, its energy dependence and its impact on strain measurements are known for a long time [64,65], it has more recently been systematically investigated by combining high-precision, energy-dependent experiments with FLUX simulations (see below), using an AlInN thin film on a GaN substrate as a model system [66]. Whereas, as expected, the angular scan exhibits only one dip in the AlInN signal, two minima are found for the GaN substrate: one at the expected position for relaxed (i.e. bulk) GaN, and one at the angular position of the thin film axis (Fig. 13). The latter peak, which is due to ions which were steered across the interface into the (misaligned) GaN axis, becomes less pronounced as the beam energy increases. However, it should be stressed that its intensity is still very significant at 2 MeV, i.e. a standard energy value in many labs. Additionally, comparison of the experimental data to FLUX simulations reveals that the steering effect not only generates a second peak, but also shifts the position of the main peak – thus resulting in an erroneous strain measurement. As shown by Lorenz et al., simulations are thus crucial to deduce the correct strain value [66].

3.5. Impurity lattice location

Since many decades, researchers have been intensively searching for techniques to accurately determine the lattice site of impurities in crystals. These impurities can be both detrimental (e.g., creating deep centers in the bandgap of a semiconductor) or beneficial (e.g., electrical, optical, magnetic... doping). The exact position occupied by the impurity in the host lattice will determine whether or not it is active as a deep center or dopant. From the early days of channeling, it became clear that this technique is ideally suited to *directly* determine lattice positions in single crystals, i.e. without the need for sophisticated modeling, as is required to interpret the data obtained by other suitable techniques as

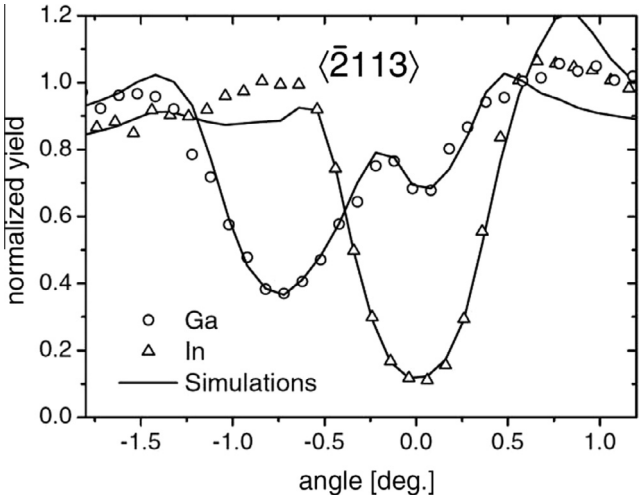

Fig. 13. 2 MeV angular scans for In (InGaN thin film) and Ga (GaN substrate), along with Monte Carlo simulations (see text for explanation). Reproduced from [66].

extended X-ray absorption fine structure [EXAFS], Mössbauer spectroscopy, perturbed angular correlation... [67].

Although in most crystals, impurities can assume a whole zoo of different positions [68], the methodology will be illustrated by focusing on two main categories: *substitutional* sites (i.e. impurities replacing a host lattice atom) and *interstitial* sites (impurities occupying any other position in the host crystal). The latter can be either *regular* or *random* interstitials. In the simplest approach, substitutional impurities contribute to the channeling behavior in a similar way as the host atoms do, whereas interstitial impurities do not share the crystallographic symmetry of the host crystal and consequently result in dechanneling (Fig. 14) [39]. Hence, the yield of violent-collision nuclear processes (backscattering, nuclear reaction, X-ray emission...) should provide a quantitative measure of the non-substitutional fraction.

In fact, in their early studies of Sb-implanted Si (see Section 3.1), Davies and Mayer not only observed channeling in the Si substrate – from which they could determine the formation and recovery of defects – but in the Sb signal as well [36]. From this observation they concluded that Sb is positioned along the row of Si atoms. However, they realized that in order to fully determine the lattice site, a measurement along one crystallographic direction is insufficient. Indeed, from the channeling behavior, one only deduces displacements away from the atomic row in the direction *perpendicular* to the axis. Therefore, the authors performed channeling experiments along two major axes, *in casu* ⟨111⟩ and ⟨110⟩. From the fact that both geometries exhibited channeling, they concluded that Sb occupies substitutional sites. Since then, channeling has become a routine technique to determine the position of impurities in single crystalline hosts, making optimal use of the inherent strengths of the ion beam technique, such as mass resolution, depth resolution, element or isotope selectivity, high sensitivity to low concentrations, etc. The substitutional fraction can be directly deduced from a comparison of the minimum yield in the host (χ_{min}^{host}) and impurity (χ_{min}^{imp}) signal, respectively:

$$f_s^{imp} \approx 1 - \frac{\chi_{min}^{imp} - \chi_{min}^{host}}{1 - \chi_{min}^{host}} \quad (5)$$

However, the great care the authors took in what is often considered the first channeling lattice location study [36], is unfortunately no longer systematically followed. Plenty of studies claim substitutionality from merely one measurement, most often along the axis perpendicular to the sample surface. This potential pitfall is best illustrated by the textbook-example study of Yb-doped Si [69]. Indeed, Andersen et al. observed excellent channeling effects in both the Si crystal and the Yb signal when aligning the ion beam along either the ⟨100⟩ or ⟨111⟩ direction. Hence, one is inclined to positively confirm the substitutional position of Yb. However, when repeating the experiment along the ⟨110⟩ direction, rather than a reduction of the Yb backscattering yield, a significant enhancement was observed, to a value largely exceeding the yield of a random measurement – whereas the channeling effect in the Si signal remained unaffected (Fig. 15)! Putting the results of the three measurements together, it was concluded that Yb occupies a position in the center of the conventional diamond unit cell, i.e. in the center of the 'empty cage'. Whereas this is a highly symmetric site, it is not a substitutional position since the impurity does not replace a host atom – resulting in channeling along several directions (e.g., ⟨100⟩, ⟨111⟩...), but not along all of them (e.g., ⟨110⟩). The fact that the yield largely exceeds the value expected for random incidence has been explained by the flux peaking effect [69–71], i.e. the channeling effect itself focuses the He ions towards the middle of the axial Si channels, exactly where the Yb atoms reside, resulting in a higher scattering probability. In conclusion, measuring along several independent directions is absolutely indispensable for accurate lattice location.

A specific strength of channeling is that the respective site occupations can be *quantitatively* determined. From a comparison of

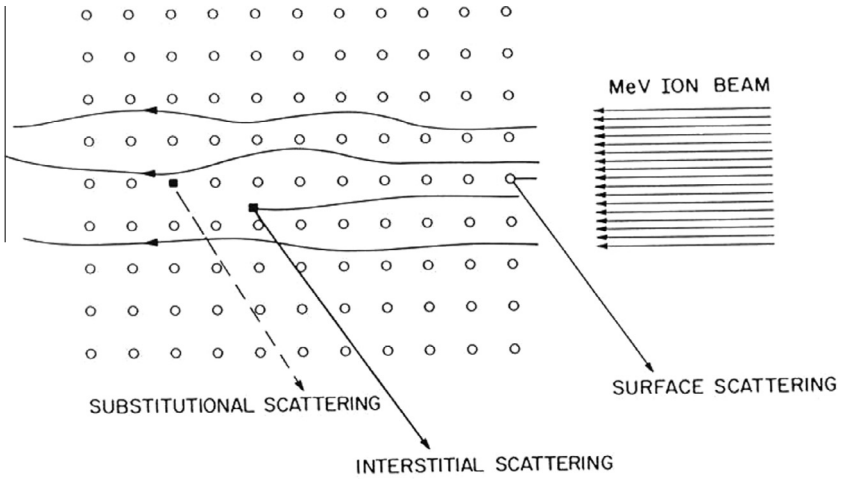

Fig. 14. Schematic of channeling trajectories and the interaction of the channeled ions with surface atoms and substitutional and interstitial impurities. Reproduced from [39].

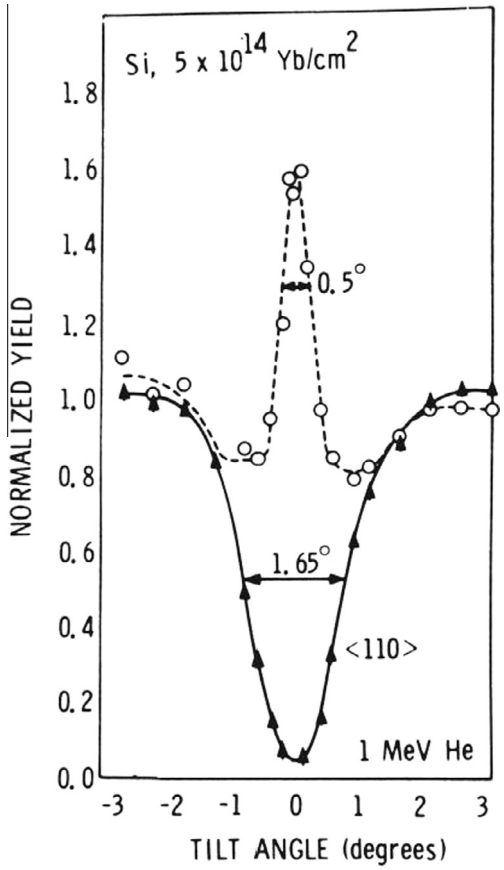

Fig. 15. 1 MeV He angular scan along the ⟨1 1 0⟩ direction for Yb-implanted Si. Reproduced from [69].

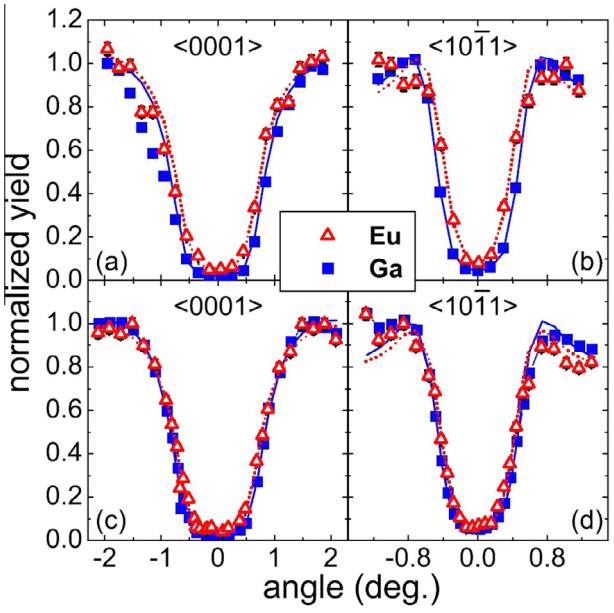

Fig. 16. Experimental (symbols) and fitted (lines) angular scans for Eu-implanted GaN along a perpendicular (a and c) and non-normal (b and d) axis, after annealing at 900 °C (a and b) and 1000 °C (c and d). Reproduced from [73].

yield reduction in the impurity signal to the one in the host signal (reflecting the crystalline quality of the host), the substitutional fraction can be easily calculated (Eq. (5)). This is by far the simplest approach, and the one most frequently used. However, as pointed out above, one should be particularly careful when limiting the experiment to (i) merely one channeling geometry and/or (ii) just a random and aligned spectrum.

On the other hand, recording the *full angular scan* provides a wealth of extra information. Both the minimum yield and (particularly!) the critical angle are very sensitive to minor displacements from the ideal site. These displacements can be static or dynamic (i.e. an increased vibration amplitude). Small displacements will typically result in a narrowing of the channeling dip, whereas large displacements (ultimately towards the middle of the channel) result in significantly enhanced yields as well, as illustrated above for the ⟨1 1 0⟩ scan of Yb-doped Si (Fig. 15).

Although such angular scans contain very valuable and detailed information on the *exact* lattice positions, it requires computer simulations to extract accurate quantitative numbers. One very successful code is FLUX [72], a Monte Carlo program which treats the nearby atoms in a binary collision model whereas the surrounding atoms are considered as continuum strings, and furthermore takes impact-parameter dependent electron interactions as well as (correlated) thermal lattice vibrations into account. As an example, Fig. 16 shows the ⟨0 0 0 1⟩ and 10$\bar{1}$1 scans of Eu-doped GaN [73]. At first glance, the nearly coinciding profiles of Eu and Ga infer nearly perfect substitutionality of Eu. However, careful analysis with the FLUX code clearly indicates that the Eu atoms are displaced by ~0.24 (3) Å along the direction of the *c*-axis for a sample annealed at 900 °C. Upon further annealing at 1000 °C, full incorporation of the Eu dopants into the Ga sites occurs. Considering the vast amount of lattice location studies using ion channeling, there is undoubtedly a great opportunity for more frequent use of such simulation codes, hence fully exploiting the wealth of information which is contained in the experimental data.

But was the pioneering work by Davies and Mayer [36] really the first lattice location study? Actually it wasn't: already in 1965, Domeij and Björkvist determined the lattice site of Rn in W, using a different approach to channeling [24]. Inspired by the earlier work using the Al(p,γ)Si resonance induced with an external proton beam [20], they conducted a similar experiment with charged particles originating from *within* the crystal. To this end, they implanted a very low fluence of radioactive ^{222}Rn into a W ⟨1 1 1⟩ crystal. The subsequent decay of these radioactive isotopes to ^{218}Po is accompanied by the emission of an α particle with an energy of 5.49 MeV. As explained in Section 2.3, according to the rule of reversibility, these α particles undergo exactly the same channeling as those of an external ion beam impinging on a crystal, hence also revealing the lattice site of the (α-emitting) impurity. Consequently, the first lattice site study applied what is now known as *emission channeling*. The experimental conditions were very simple (using wedges instead of a goniometer to change the direction between the crystal axes and the detector) but clearly showed very pronounced channeling effects, from which a substitutional lattice site could be determined.

In the following decades, emission channeling seemed largely forgotten for a long time, until it revived in the 80s, with major efforts by Lindner, Hofsäss and Wahl (see Refs. [31,32,68] for reviews on emission channeling). In particular, the use of (i) two-dimensional position-sensitive detectors [33] and (ii) detailed simulation codes greatly enhanced the sensitivity and accuracy of the technique, respectively. Later on, in the 90s, electron emitting isotopes were largely exploited as well [68,33]. Being charged particles, electrons undergo a similar channeling effect along crystallographic directions – except that the potential is attractive rather than repulsive (due to the negative charge) and that the analytical treatment is done in a quantum mechanical and relativistic way. To this end, Hofsäss and Lindner developed the "Many-beam" computer code [31], based on the same approach as used in

transmission electron microscopy. Typically, the two-dimensional channeling pattern is simulated for a specific impurity/host combination and for a large number of possible impurity sites, as well as for displacements from these ideal sites. Finally, a fit of the two-dimensional experimental pattern to the simulations allows to deduce the lattice site(s) occupied by the impurities. Obviously, the availability of a beam of radioactive isotopes with suitable half-life and a suitable energy of the emitted particles remains a bottleneck for emission channeling. Currently, most of the experiments are performed at the ISOLDE facility in Cern, where the first successful *on line* emission channeling measurements were lately done [74,75], very recently even while measuring during the radioactive implantation [76].

One of the major advantages of emission channeling is that the captured data solely originate from the radioactive impurity, hence showing no substrate signal. Therefore, this approach is extremely suitable to investigate the lattice site of low concentrations of light impurities in heavy matrices, a combination which is virtually impossible with RBS/channeling. Moreover, the sensitivity and accuracy obtained when using a PSD and proper data analysis allow resolving minor fractions, even in the presence of a much larger fraction which dominates the spectra [77,78].

As an example of the latter, Fig. 17 shows emission channeling patterns after implanting radioactive ^{56}Mn implanted into GaN [78]. Panels (a)–(d) are two-dimensional emission patterns collected in the vicinity of four major crystal axes, with the color representing the yield. From these patterns, the crystal symmetry is clearly revealed, with the major planes intersecting along the axial direction. Experimental data were captured along 4 axes (i.e. more than strictly needed to determine the lattice site, thus enhancing the accuracy of the analysis) and compared to simulations using the Many-beam formalism. In these simulations, the authors considered probes located in the wurtzite lattice on substitutional Ga (S_{Ga}) and N (S_N) sites with varying rms-displacements, a number of interstitial sites, i.e. tetrahedral (T), octahedral (O), hexagonal (H), bondcentered (BC) and antibonding (AB), as well as interstitial sites resulting from displacements along the *c* or the basal directions. For all four directions, the best agreement was obtained for Mn atoms replacing Ga, as is expected from their chemical similarity. However, when allowing a second site, a fit with S_{Ga} and S_N double occupancy (Fig. 17e–h) consistently gives the best fit compared to any other combination of sites or to the S_{Ga} single occupancy. The optimal site occupancy is 81% S_{Ga} and 19% S_N. The sensitivity of this approach is illustrated in Fig. 18, which shows the reduced χ^2 of the fit as the second (non-S_{Ga}) site is moved along the *c*-axis between two neighboring S_{Ga} sites, i.e. also assuming AB, T, S_N and BC sites. As soon as the Mn impurity is displaced a few tenths of an Å away from the S_N antisite, the

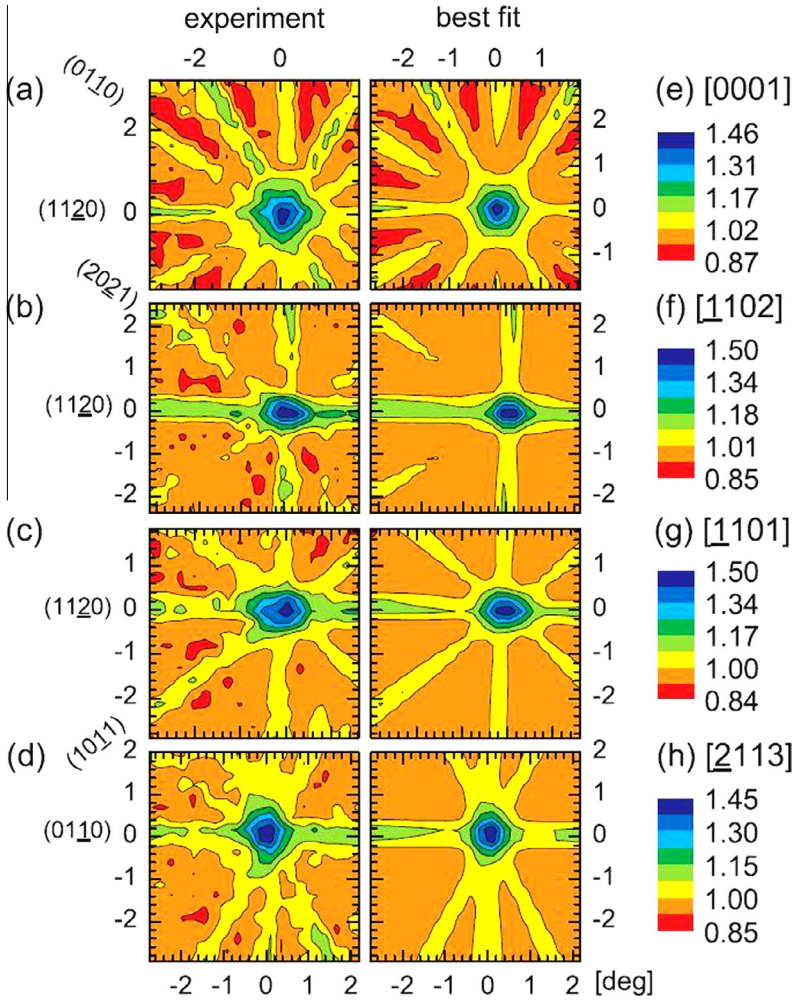

Fig. 17. Normalized ^{56}Mn(GaN) emission channeling patterns in the vicinity of 4 different axes: (a–d) experimental patterns; (e–h) best fits corresponding to 81% and 19% Mn on S_{Ga} and S_N sites, respectively. Reproduced from [78].

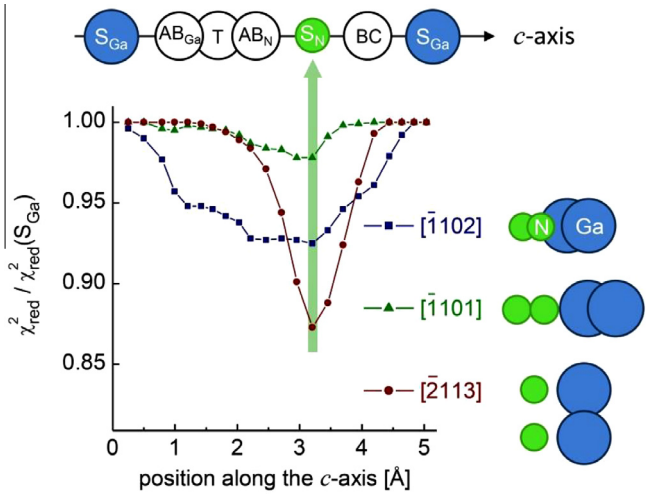

Fig. 18. Reduced χ^2 of the fits for ^{56}Mn(GaN) using two sites, i.e. S_{Ga} and an intermediate position along the *c*-axis (see schematic on top). Reproduced from [78].

χ^2 of the fit significantly increases, in particular for the [2 1 1 3] axis, which is the most sensitive direction to distinguish between Ga and N rows [78].

3.6. Mosaic spread

Obviously, the entire discussion so far silently assumed a perfectly single-crystalline host. Any deviation from such ideal crystallinity will significantly impact the channeling behavior. This is already clear from the equation used to calculate the substitutional fraction (Eq. (5)) which includes the substrate minimum yield. A specific example of non-ideal crystallinity is mosaic spread, whereby the crystal consists of individual grains which are slightly misoriented with respect to one another. As a consequence, the position of the axial and planar directions is no longer uniquely defined, but slightly varies over an amount which can be equal to or even larger than the ion beam divergence (i.e. a few tenths of a degree). In this case, the channeling effect is "smeared out" over a wider angular range of alignment, and the angular scans become broader and less deep. This smearing-out is clearly illustrated in the two-dimensional (emission) channeling pattern along the [1̄ 1 0 1] axis of ^{167m}Er implanted in AlN, a material that often suffers from severe mosaicity [79,80]. As shown in Fig. 19, the typical planar directions normally visible in channeling patterns (cf. Fig. 17) are replaced by a blurry "hump" and the "best fit", with only 22% of the Er on a regular site, does not agree well with the experimental pattern [80]. Moreover, the measurements along 4 independent axes could no longer by consistently fitted: the obtained substitutional fraction decreases as the angle between the measured axis and the surface normal increases. However, a detailed XRD study of the mosaic structure of the samples, taking not only the *tilt* of the grains into account, but also their in-plane *twist* [81], allows to incorporate the real sample structure in the simulation code. Using this approach, good fits to the experimental data are obtained (Fig. 19), yielding the same value for the substitutional fraction for all 4 axes, approximately 60% in this example. This approach is possible for all channeling experiments, including RBS/channeling, as long as quantitative information on the mosaic structure (i.e. the tilt and twist) is available for each sample.

3.7. Thermal vibrations

Already in Lindhard's model [17], it was shown how vibrations have a direct impact on the values of the minimum yield and the critical angle (see Section 2.3). Hence, thorough knowledge of the vibrational properties of the sample (including its impurities) is crucial for good analysis or modeling – a non-trivial challenge! This can be of particular importance when determining the lattice site of impurities, since their vibrational amplitude can differ significantly from that of the host atoms. In most cases, thermal vibrations are incorporated using, e.g., the Debye model. Considering the simplifying assumptions of that model as well as the fact that it averages over the crystal, it would be worthwhile to explore the incorporation of *ab initio* calculated phonon spectra, which are known to be more accurate in many cases.

From the experimental point of view, the thermal vibration amplitude can be easily tuned by varying the sample temperature. Whereas the channeling effect will ultimately completely vanish at elevated temperature, when lowering the temperature (which is not trivial when using a high-precision goniometer) the minimum yield decreases while the critical angle increases – in a way already predicted by Lindhard's theory [17] and refined by Barrett's computer simulations [41]. This effect, which was already experimentally demonstrated by the early blocking experiments of Tulinov et al. [25], has been regularly used to study phonon-related properties, a beautiful example of which is Lynn Rehn's investigation of high-temperature superconductors.

When measuring the width of the [0 0 1] angular scan of $(Bi_{1.7}Pb_{0.3})Sr_2CaCu_2O_x$ single crystals as a function of decreasing temperature, an overall increase as expected from Barrett's formalism is observed [82,83]. Fig. 20 shows this behavior for three integration windows, representing the Bi–Pb, Bi–Pb–Sr and Bi–Pb–Sr–Cu signal, respectively. However, at the critical temperature for superconductivity (T_c = 90 K) a very sudden jump in width is observed for the scans of the integration window containing the Cu signal. Further PIXE measurements confirmed that an abrupt transition in the channeling width occurs for Cu. As such, this behavior may not be surprising since superconductivity

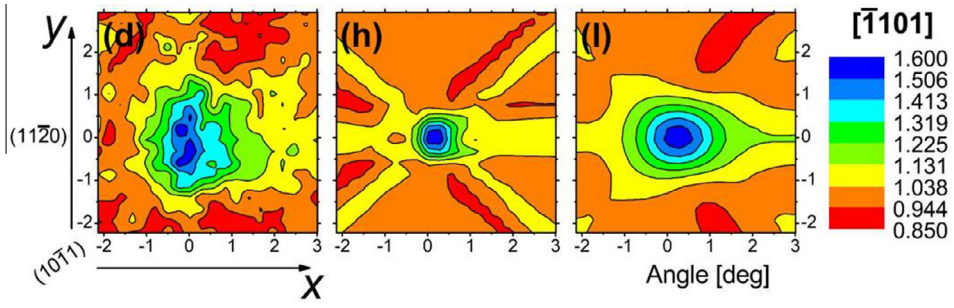

Fig. 19. Normalized ^{167m}Er(AlN) emission channeling patterns in the vicinity of the ⟨1̄ 1 0 1⟩ axis: experimental pattern from a sample with mosaic structure (left); "best fit" when assuming a perfect crystal (middle); and fit taking the mosaicity into account (right). Reproduced from [80].

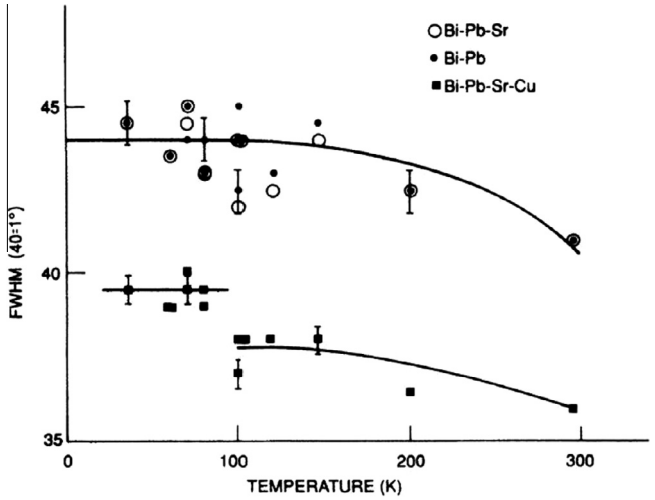

Fig. 20. FWHM of the ⟨001⟩ RBS angular scans of $(Bi_{1.7}Pb_{0.3})Sr_2CaCu_2O_x$, as a function of temperature. Three integration windows were used, each representing a different combination of elements. Reproduced from [82].

(and Cooper pairs in particular) is a phonon-mediated phenomenon. However, once again, it is the element specificity of the ion beam techniques that allows to unravel the specific role of Cu in the superconductivity.

3.8. . . .and much more!

As outlined in the beginning, this paper primarily focuses on RBS/channeling, largely ignoring alternatives based on NRA or PIXE. Among the many topics which were not mentioned, is for instance the characterization of nanoscale materials, e.g., nanowires and (embedded) quantum dots [84]. While these systems typically have a dimension which is (much) smaller than the depth resolution of the ion beam analysis technique, very valuable *integral* information can be obtained, a.o. by cleverly designing the experiment and the sample structure. Examples are the strain in multiple quantum wells (very comparable to the experiments by W.K. Chu et al. and Selen et al. described in Section 3.4) or the crystallinity and elastic strain in buried nm-size quantum dots. Since the size of these systems is much smaller than the wavelength of the channeled ion, simulations are indispensable for a correct interpretation of the angular scans [85].

Alternatively, using channeling in combination with high-resolution RBS allows to drastically improve the depth resolution. This can for instance be achieved by using magnetic spectrometers (as was actually done in the very first experiments in the late 50s), eventually at low or medium energy, ultimately achieving monolayer depth sensitivity, as shown by Kimura et al. [86]. On the other hand, high lateral resolution is obtained by transmission channeling using a nuclear microprobe proton beam, and is powerful in detecting defects such as dislocations, stacking faults, precipitates, etc. [87]. From the energy loss of the transmitted protons, the distribution of the defects can be deduced [88].

Finally, channeled implantation is briefly mentioned, hence going back to where it all started: channeling of low-energy heavy ions. Channeled implantation has proven very beneficial to reduce sputtering as well as the damage induced during ion implantation. In particular when implanting very heavy ions, this approach may be crucial to avoid sample amorphization or self-sputtering. Typical implantation conditions, i.e. medium ion masses and energies of tens of keV, result in critical angles as large as 3–6°, making good alignment feasible without the need for a high-precision goniometer. However, one should keep in mind that Eq. (1) is no longer valid under these conditions. Indeed, Lindhard's 1965 channeling paper [17] already pointed out that for low-energy, high-mass ions, the critical angle for channeling is given by

$$\Psi_c = \sqrt{\frac{Ca}{d\sqrt{2}}}\Psi_1 \tag{6}$$

where ψ_1 is the critical angle for high-energy light particles (Eq. (1)) and C is a constant. Channeled implantation, including its temperature dependence, has been studied experimentally and compared to MDrange simulations [89,90], and shown of crucial importance in specific ion beam synthesis [91] and doping [92] studies.

4. Conclusion

Clearly, the past 50 years of channeling have been really exciting, not only in terms of its applications in materials science, but also for the physics of channeling itself. Throughout these 5 decades, ion channeling has developed to a workhorse technique to study a wide variety of properties related to (a deviation of) the sample crystallinity. Consequently, after 50 years, we can consider channeling as a very mature technique.

However, as touched upon in this paper, there are still plenty of challenging opportunities, three of which will be briefly commented on a little more. Firstly, it has been shown that simulations can add significantly to the data interpretation, in particular to provide quantitative information. This approach has been shown crucial when performing accurate lattice location studies (e.g., using the FLUX or Many-beam codes), but also for assessing defects (e.g., McChasy). Despite the fact that a combination of high-precision experiments and detailed simulations is extremely powerful, its use has not been all that widespread, and there is clearly more effort needed to maximally distill the information hidden in the experimental data. Ideally, of course, one would like to see very user-friendly programs, as are widely available to simulate implantation profiles (e.g., SRIM) or Rutherford backscattering spectra (RUMP, SIMNRA, NDF, Corteo. . .). Such programs would be very helpful in carefully designing the optimal experiments as well.

Computational approaches may also be very helpful on very different levels. For instance, current *ab initio* techniques allow to calculate both the phonon spectrum and the (screened!) potential of a crystal, as opposed to the approximated models that are typically used in channeling analysis. How important the use of *ab initio* potentials would be, compared to the typical combination of screened Coulomb potentials and continuum potentials, needs to be investigated. Particularly for ionic crystals the effect may become significant.

Finally, on the instrumental side, further improvement of the detection system would be beneficial. In this context, trying to improve the energy resolution is just one (obvious) aspect. Besides, as illustrated above, a more widespread use of position sensitive detectors could both boost the experimental throughput and improve the sensitivity. However, the rather limited energy resolution of the detectors which are currently commercially available remains inferior to what is acceptable for many experiments.

Overall, channeling is complementary to many other characterization techniques used to investigate crystalline materials, and often goes hand in hand with them. While these techniques may sometimes be simpler, easier or better, channeling outperforms them in many cases – in particular, due to the strengths of the specific ion beam analysis technique used, which provides depth information, element or isotope specificity, etc.; information which is often unattainable by other experimental approaches. Hence, we should not be tempted to try solving "all problems" with channeling, because we happen to have the equipment and the expertise.

Sometimes, other techniques are either easier or better – or both! Conversely, we should focus on the unique strength of channeling and fully exploit the inherent strength and power of the ion beam technique it is based on, i.e. where channeling can make the difference.

References

[1] J. Stark, Phys. Z. 13 (1912) 973.
[2] J. Stark, G. Wendt, Annal. Phys. 38 (1912) 921.
[3] J.A. Davies, G. Amsel, J.W. Mayer, Nucl. Instrum. Methods B 64 (1992) 12.
[4] P.K. Rol, J.M. Fluit, J. Kistemaker, J. Phys. 26 (1960) 1000.
[5] J.M. Fluit, P.K. Rol, J. Kistemaker, J. Appl. Phys. 34 (1963) 690.
[6] R.S. Nelson, M.W. Thompson, Phys. Lett. 2 (1962) 124.
[7] J.A. Davies, G.A. Sims, Can. J. Chem. 39 (1961) 601.
[8] M.M. Bredov, I.M. Okuneva, Sov. Phys. Dokl. 113 (1957) 795.
[9] J.A. Davies, J.D. McIntyre, G.A. Sims, Can. J. Chem. 40 (1962) 1605.
[10] M.T. Robinson, O.S. Oen, Conf. Proc. "Le Bombardement Ionique", Paris, 1962.
[11] M.T. Robinson, O.S. Oen, Appl. Phys. Lett. 2 (1963) 30.
[12] M.T. Robinson, O.S. Oen, Phys. Rev. 132 (1963) 2385.
[13] G.R. Piercy, M. Mccargo, F. Brown, J.A. Davies, Phys. Rev. Lett. 10 (1963) 399.
[14] H. Lutz, R. Sizmann, Phys. Lett. 5 (1963) 113.
[15] R.S. Nelson, M.W. Thompson, Philos. Mag. 8 (1963) 1677.
[16] G. Dearnaley, IEEE Trans. Nucl. Sci. 11 (1964) 249.
[17] J. Lindhard, Mat. Fys. Medd. Dan. Vid. Selsk. 34 (1965) 1.
[18] C. Lehmann, G. Leibfried, J. Appl. Phys. 34 (1963) 2821.
[19] J. Lindhard, Phys. Lett. 12 (1964) 126.
[20] E. Bøgh, J.A. Davies, K.O. Nielsen, Phys. Lett. 12 (1964) 129.
[21] M.W. Thompson, Phys. Rev. Lett. 13 (1964) 756.
[22] B. Domeij, Nucl. Instrum. Methods 38 (1965) 207.
[23] W. Brandt, J.M. Khan, D.L. Potter, R.D. Worley, H.P. Smith, Phys. Rev. Lett. 14 (1965) 42.
[24] B. Domeij, K. Björkqvist, Phys. Lett. 14 (1965) 127.
[25] A.F. Tulinov, V.S. Kulikauskas, M.M. Malov, Phys. Lett. 18 (1965) 304.
[26] D.S. Gemmell, R.E. Holland, Phys. Rev. Lett. 14 (1965) 945.
[27] J.U. Andersen, Mat. Fys. Medd. Dan. Vid. Selsk. 52 (2006) 655.
[28] E. Bøgh, E. Uggerhøj, Phys. Lett. 17 (1965) 116.
[29] E. Bøgh, E. Uggerhøj, Nucl. Instrum. Methods 38 (1965) 216.
[30] A.F. Tulinov, B.G. Akhmetova, A.A. Puzanov, A.A. Bednyakov, JETP Lett. 2 (1965) 30.
[31] H. Hofsäss, G. Lindner, Phys. Rep. 201 (1991) 121.
[32] U. Wahl, Phys. Rep. 280 (1997) 145.
[33] U. Wahl, J.G. Correia, A. Czermak, S.G. Jahn, P. Jalocha, J.G. Marques, A. Rudge, F. Schopper, J.C. Soares, A. Vantomme, et al., Nucl. Instrum. Methods A 524 (2004) 245.
[34] P.A. Miranda, U. Wahl, N. Catarino, M.R. da Silva, E. Alves, Nucl. Instrum. Methods A 760 (2014) 98.
[35] J.W. Mayer, L. Eriksson, S.T. Picraux, J.A. Davies, Can. J. Phys. 46 (1968) 663.
[36] J.A. Davies, J. Denhartog, L. Eriksson, J.W. Mayer, Can. J. Phys. 45 (1967) 4053.
[37] C. Erginsoy, H.E. Wegner, W.M. Gibson, Phys. Rev. Lett. 13 (1964) 530.
[38] E. Bøgh, Phys. Rev. Lett. 19 (1967) 61.
[39] L.C. Feldman, J.W. Mayer, S.T. Picraux, Materials Analysis by Ion Channeling – Submicron Crystallography, Academic Press, New York, 1982.
[40] A. Dygo, A. Turos, Phys. Rev. B 40 (1989) 7704.
[41] J.H. Barrett, Phys. Rev. B 3 (1971) 1527.
[42] A. Turos, P. Jozwik, L. Nowicki, N. Sathish, Nucl. Instrum. Methods B 332 (2014) 50.
[43] J.F. Ziegler, J.P. Biersack, U. Littmark, The Stopping and Ranges of ions in Solids, Pergamon, New York, 1985.
[44] E. Kótai, Nucl. Instrum. Methods B 85 (1994) 588.
[45] E. Albertazzi, M. Bianconi, G. Lulli, R. Nipoti, M. Cantiano, Nucl. Instrum. Methods B 118 (1996) 128.
[46] N.P. Barradas, K. Arstila, G. Battistig, M. Bianconi, N. Dytlewski, C. Jeynes, E. Kotai, G. Lulli, M. Mayer, E. Rauhala, et al., Nucl. Instrum. Methods B 262 (2007) 281.
[47] G. Bai, M.-A. Nicolet, J.E. Mahan, K.M. Geib, Phys. Rev. B 41 (1990) 8603.
[48] A. Vantomme, U. Wahl, M.F. Wu, S. Hogg, H. Pattyn, G. Langouche, H. Bender, Nucl. Instrum. Methods B 136 (1998) 471.
[49] D. Benzeggouta, I. Vickridge, Handbook on Best Practice for Minimising Beam Induced Damage during IBA, arXiv:1303.3171 [cond-mat.mtrl-sci], 2011.
[50] D.N. Jamieson, R.A. Brown, C.G. Ryan, J.S. Williams, Nucl. Instrum. Methods B 54 (1991) 213.
[51] M. Piette, F. Bodart, Nucl. Instrum. Methods B 54 (1991) 204.
[52] R.A. Brown, J.C. McCallum, J.S. Williams, Nucl. Instrum. Methods B 54 (1991) 197.
[53] D.S. Gemmell, Rev. Mod. Phys. 46 (1974) 129.
[54] J. Dekoster, H. Bemelmans, J. De Wachter, R. Moons, G. Langouche, Appl. Phys. Lett. 65 (1994) 1224.
[55] F.W. Saris, W.K. Chu, C.A. Chang, R. Ludeke, L. Esaki, Appl. Phys. Lett. 37 (1980) 931.
[56] J.C. Barbour, S.T. Picraux, B.L. Doyle, Mater. Res. Soc. Symp. Proc. 107 (1988) 269.
[57] M.F. Wu, A. Vantomme, G. Langouche, H. Vanderstraeten, Y. Bruynseraede, Nucl. Instrum. Methods B 54 (1991) 444.
[58] M.F. Wu, A. Vantomme, G. Langouche, K. Maex, H. Vanderstraeten, Y. Bruynseraede, Appl. Phys. Lett. 57 (1990) 1973.
[59] M.F. Wu, C.C. Chen, D.Z. Zhu, S.Q. Zhou, A. Vantomme, G. Langouche, B.S. Zhang, H. Yang, Appl. Phys. Lett. 80 (2002) 4130.
[60] W.K. Chu, J.A. Ellison, S.T. Picraux, R.M. Biefeld, G.C. Osbourn, Phys. Rev. Lett. 52 (1984) 125.
[61] S.T. Picraux, W.K. Chu, W.R. Allen, J.A. Ellison, Nucl. Instrum. Methods B 15 (1986) 306.
[62] L.J.M. Selen, F.J.J. Janssen, L.J. van IJzendoorn, M.J.J. Theunissen, P.J.M. Smulders, M.J.A. de Voigt, Nucl. Instrum. Methods B 161 (2000) 492.
[63] L.J.M. Selen, F.J.J. Janssen, L.J. van IJzendoorn, M.J.J. de Voigt, P.J.M. Smulders, M. J.A. Theunissen, Nucl. Instrum. Methods B 184 (2001) 559.
[64] W.K. Chu, C.K. Pan, C.A. Chang, Phys. Rev. B 28 (1983) 4033.
[65] S. Hashimoto, Y.Q. Feng, W.M. Gibson, L.J. Schowalter, B.D. Hunt, Nucl. Instrum. Methods B 13 (1986) 45.
[66] K. Lorenz, N. Franco, E. Alves, I.M. Watson, R.W. Martin, K.P. O'Donnell, Phys. Rev. Lett. 97 (2006).
[67] A. Vantomme, B. De Vries, U. Wahl, Lattice Location of RE Impurities in III-Nitrides, in: Rare Earth Doped III-Nitrides for Optoelectronic and Spintronic Applications, Top. Appl. Phys. 124 (2010) 55.
[68] U. Wahl, Hyp. Int. 129 (2000) 349.
[69] J.U. Andersen, O. Andreasen, J.A. Davies, E. Uggerhøj, Radiat. Effects 7 (1971) 25.
[70] F.H. Eisen, E. Uggerhøj, Radiat. Effects 12 (1972) 233.
[71] D. Van Vliet, Radiat. Effects 10 (1971) 137.
[72] P.J.M. Smulders, D.O. Boerma, Nucl. Instrum. Methods B 29 (1987) 471.
[73] K. Lorenz, E. Alves, I.S. Roqan, K.P. O'Donnell, A. Nishikawa, Y. Fujiwara, M. Bockowski, Appl. Phys. Lett. 97 (2010).
[74] S. Decoster, S. Cottenier, U. Wahl, J.G. Correia, L.M.C. Pereira, C. Lacasta, M.R. Da Silva, A. Vantomme, Appl. Phys. Lett. 97 (2010) 151914.
[75] L.M.C. Pereira, U. Wahl, S. Decoster, J.G. Correia, L.M. Amorim, M.R. da Silva, J.P. Araújo, A. Vantomme, Phys. Rev. B 84 (2011) 125204.
[76] L.M. Amorim, U. Wahl, L.M.C. Pereira, S. Decoster, D.J. Silva, M.R. da Silva, A. Gottberg, J.G. Correia, K. Temst, A. Vantomme, Appl. Phys. Lett. 103 (2013).
[77] U. Wahl, A. Vantomme, J. De Wachter, R. Moons, G. Langouche, J.G. Marques, J. G. Correia, Phys. Rev. Lett. 79 (1997) 2069.
[78] L.M.C. Pereira, U. Wahl, J.G. Correia, S. Decoster, L.M. Amorim, M.R. da Silva, J.P. Araújo, A. Vantomme, Phys. Rev. B 86 (2012) 195202.
[79] B. De Vries, V. Matias, A. Vantomme, U. Wahl, E.M.C. Rita, E. Alves, A.M.L. Lopes, J.G. Correia, Appl. Phys. Lett. 84 (2004) 4304.
[80] B. De Vries, U. Wahl, S. Ruffenach, O. Briot, A. Vantomme, Appl. Phys. Lett. 103 (2013).
[81] V. Srikant, J.S. Speck, D.R. Clarke, J. Appl. Phys. 82 (1997) 4286.
[82] L.E. Rehn, R.P. Sharma, P.M. Baldo, Y.C. Chang, P.Z. Jiang, Phys. Rev. B 42 (1990) 4175.
[83] L.E. Rehn, Nucl. Instrum. Methods B 64 (1992) 161.
[84] E. Alves, M. Breese, Nanoscale Materials Defect Characterization, in: Ion Beams in Nanoscience and Technology, Springer-Verlag, Berlin, 2009, p. 185.
[85] A. Fonseca, E. Alves, J.P. Leitao, N.A. Sobolev, M.C. Carmo, A.I. Nikiforov, Mater. Sci. Eng. B 124 (2005) 462.
[86] K. Kimura, K. Ohshima, M. Mannami, Appl. Phys. Lett. 64 (1994) 2232.
[87] M.B.H. Breese, D.N. Jamieson, P.J.C. King, Materials Analysis using a Nuclear Microprobe, Wiley, New York, 1996.
[88] P.J.C. King, M.B.H. Breese, P.J.M. Smulders, P.R. Wilshaw, G.W. Grime, Phys. Rev. Lett. 74 (1995) 411.
[89] S.M. Hogg, B. Pipeleers, A. Vantomme, M. Swart, Appl. Phys. Lett. 80 (2002) 4363.
[90] S.M. Hogg, A. Vantomme, M.F. Wu, B. Pipeleers, M. Swart, Nucl. Instrum. Methods B 175 (2001) 585.
[91] M.F. Wu, A. Vantomme, H. Pattyn, G. Langouche, Appl. Phys. Lett. 67 (1995) 3886.
[92] A. Vantomme, S.M. Hogg, M.F. Wu, B. Pipeleers, M. Swart, S. Goodman, D. Auret, K. Iakoubovskii, G.J. Adriaenssens, K. Jacobs, et al., Nucl. Instrum. Methods B 175 (2001) 148.